A Journal of the Gesellschaft Deutscher Chemiker

Angewandte International Edition GDCh Chemie

www.angewandte.org

Accepted Article

Title: Two-photon Clusteroluminescence Enabled by Through-Space Conjugation for In Vivo Bioimaging

Authors: Jianyu Zhang, Hanchen Shen, Zuping Xiong, Lidong Du, Moxin Li, Xinwen Ou, Xinyan Zhu, Jacky W. Y. Lam, Tzu-Ming Liu, Changhuo Xu, Haoke Zhang, and Ben Zhong Tang

To be cited as: *Angew. Chem. Int. Ed.* **2024**, e202413751

Link to VoR: https://doi.org/10.1002/anie.202413751

WILEY VCH

10.1002/anie.202413751

WILEY·VCH

COMMUNICATION

Two-photon Clusteroluminescence Enabled by Through-Space Conjugation for In Vivo Bioimaging

Jianyu Zhang,[a,b,f]† Hanchen Shen,[b]† Zuping Xiong,[a,d,e]† Lidong Du,[b,c] Moxin Li,[c] Xinwen Ou,[b] Xinyan Zhu,[b] Jacky W. Y. Lam,[b] Tzu-Ming Liu,[c] Changhuo Xu,*[c] Haoke Zhang,*[a,d,e] and Ben Zhong Tang*[a,b,g]

[a] Dr. J. Zhang, Mr. Z. Xiong, Prof. H. Zhang, and Prof. B. Z. Tang
MOE Key Laboratory of Macromolecular Synthesis and Functionalization, Department of Polymer Science and Engineering
Zhejiang University
Hangzhou 3100587, China
E-mail: zhanghaoke@zju.edu.cn

[b] Dr. J. Zhang, Dr. H. Shen, Mr. L. Du, Dr. X. Ou, Ms. X. Zhu, Dr. J. W. Y. Lam, and Prof. B. Z. Tang
Department of Chemistry, Hong Kong Branch of Chinese National Engineering Research Center for Tissue Restoration and Reconstruction
The Hong Kong University of Science and Technology
Clear Water Bay, Kowloon, Hong Kong, 999077, China
E-mail: tangbenz@cuhk.edu.cn

[c] Mr. L. Du, Ms. M. Li, Prof. T. Liu, Dr. C. Xu
MOE Frontiers Science Center for Precision Oncology, Faculty of Health Sciences
University of Macau
Macao, 999078 China
E-mail: changhuoxu@um.edu.mo

[d] Mr. Z. Xiong, Prof. H. Zhang
Zhejiang-Israel Joint Laboratory of Self-Assembling Functional Materials, ZJU-Hangzhou Global Scientific and Technological Innovation Center
Zhejiang University
Hangzhou 311215, China

[e] Mr. Z. Xiong, Prof. H. Zhang
Centre of Healthcare Materials, Shaoxing Institute, Zhejiang University
Shaoxing 312000, China

[f] Dr. J. Zhang
Stratingh Institute for Chemistry, University of Groningen
Groningen 9747 AG, The Netherlands

[g] Prof. B. Z. Tang
School of Science and Engineering, Shenzhen Institute of Aggregate Science and Technology
The Chinese University of Hong Kong
Shenzhen, Guangdong 518172, China

[†] These authors contributed equally to this work.

Supporting information for this article is given via a link at the end of the document.

Abstract: Clusteroluminescence (CL) materials without largely conjugated structures have gained significant attention due to their unique photophysical properties and potential in bioimaging. However, low luminescence efficiency and short emission wavelength limit their development. This work designs three luminogens with CL properties (CLgens) by introducing *n*-electron-involved through-space conjugation (TSC) into diarylmethane. Apart from single-photon excited long-wavelength (688 nm) and high-efficiency (29%) CL, two-photon clusteroluminescence (TPCL) is successfully achieved in such small luminogens with only two isolated heteroatomic units. TSC stabilized in the aggregate state has been proven to realize efficient spatial electron delocalization similar to conventionally conjugated compounds. Encouraged by the excellent TPCL properties, two-photon imaging of blood vessels *in vivo* and biocompatibility verification utilizing CLgens are also achieved. This work illustrates the essential role of TSC in promoting nonlinear optical properties of CLgens and may facilitate further design and development of the next generation of bioprobes with excellent biocompatibility.

Visualizing and monitoring biological structures and processes is of great significance for exploring the mysteries of biological and physical science.[1] Fluorescence technology, with its high sensitivity and spatiotemporal resolution, has become an essential tool, especially for bioprobes with high biological activity and low toxicity.[2] For example, green fluorescent protein (GFP) expressed autonomously in cells has been developed as diverse fluorescent bioprobes.[3] However, due to the large size and complex expression of the protein, GFP-based bioprobes are limited to some microenvironments and sometimes output false signals.[4] Thus, developing biocompatible fluorescent probes with simple structures and small sizes is an emerging topic. Recently, clusteroluminescence (CL) materials with nonconjugated structures, such as polyethylene glycol, polyesters, and polyamide, have gained significant attention because they can produce intrinsic luminescence in the aggregate state.[5] Unlike traditional luminogens based on through-bond conjugation (TBC) and polycyclic aromatic skeletons, luminogens with CL property (CLgens) do not contain any extended conjugated unit, making them promising bioprobes with high biocompatibility and biodegradability.[6] Additionally, the working mechanism of CLgens, based on noncovalent through-space conjugation (TSC), gives them high sensitivity to stimuli and external environments, which is advantageous for monitoring biological processes.[7]

However, since the strength of the π-electron-involved TSC is relatively weak, most reported CLgens exhibit low efficiency and short emission wavelength within the blue region, limiting their potential for biological applications.[7a, 8] Recent studies have discovered that introducing *n* electrons could significantly

10.1002/anie.202413751

enhance the strength of TSC and electron delocalization due to the high electron density of heteroatoms and formed intermolecular TSC, which enable CLgens to produce red and near-infrared (NIR) CL with high luminescence efficiency, considerably improving their photophysical properties.[5c, 9] On the other hand, realizing the two-photon excitation of organic luminogens using NIR light is of interest for many practical applications due to the low phototoxicity and deep penetration depth in biological tissues.[10] Many luminogens with two-photon fluorescence are constructed based on TBC and largely conjugated donor and acceptor groups (Figure 1a).[11] However, due to the lack of extended conjugated structures, the potential nonlinear optical properties of CLgens, such as two-photon fluorescence, have not been considered or explored. Thus, developing CLgens with two-photon excited behaviors as new bioprobes would be significant but challenging regarding fundamental photophysical theories and application values.

In this work, we demonstrate a general design strategy by introducing *n*-electron units into the diarylmethane derivatives to efficiently increase the strength of TSC. Apart from single-photon excited long-wavelength (up to 688 nm) and high-efficiency (up to 29%) CL, for the first time, we successfully achieve the two-photon clusteroluminescence (TPCL) from these CLgens with only two isolated heteroatomic units (Figure 1b). Leveraging these properties, we also demonstrate two-photon vascular imaging of mouse ears *in vivo* and high biocompatibility of the designed CLgens. It is believed that elucidation of the structure-property relationships in emerging CLgens, with unconventional nonlinear TPCL arising from TSC, could promote the development of TSC-based organic photophysics and next-generation bioprobes.

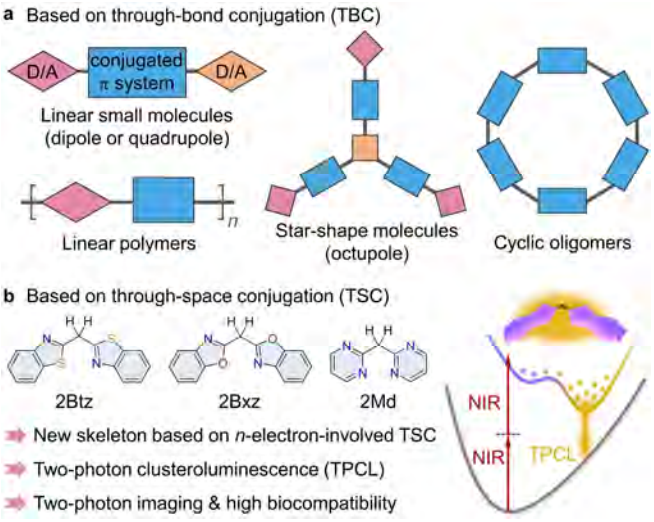

Figure 1. (a) Schematic diagram of traditional molecular skeletons with two-photon fluorescence based on through-bond conjugation, D/A = donor/acceptor groups. (b) Schematic illustration of newly designed CLgens with TSC-based two-photon clusteroluminescence under near-infrared (NIR) laser excitation.

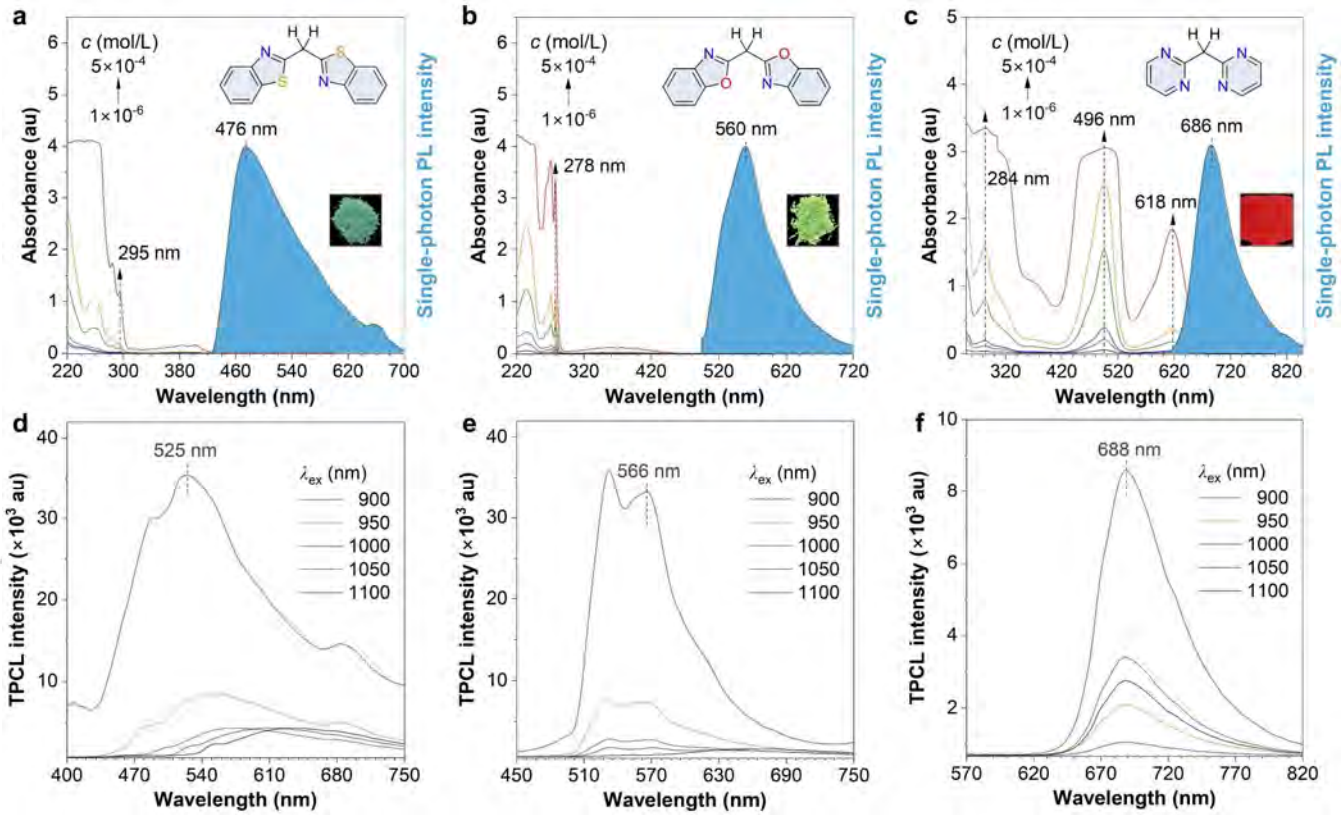

Figure 2. (a–c) Absorption spectra of (a) 2Btz, (b) 2Bxz, and (c) 2Md in ACN solutions with different concentrations and single-photon photoluminescence (PL) spectra of samples in the crystalline (2Btz and 2Bxz) or oily (2Md) state. Excitation wavelength: 390 nm for 2Btz, 470 nm for 2Bxz, and 510 nm for 2Md. Inset: chemical structures and luminescent photographs of corresponding samples under a 365 nm UV lamp. (d–f) Two-photon clusteroluminescence (TPCL) spectra of (d) solid 2Btz, (e) solid 2Bxz, and (f) oily 2Md under different excitation wavelengths.

10.1002/anie.202413751

The photophysical properties of the synthesized CLgens were first investigated. 2Btz and 2Bxz show typical maximum absorption wavelength (λ_{ab}) at 295 nm and 278 nm in dilute acetonitrile (ACN) solutions (10^{-6} mol/L), respectively, which arise from their isolated heteroatomic rings (Figure 2a and b).[12] Interestingly, new broad absorption peaks in the range of 300–400 nm are observed in 2Btz and 2Bxz when the concentration increases to 5×10^{-4} mol/L, which suggests the formation of stable TSC according to previous studies.[13] Apart from the λ_{ab} at 284 nm from isolated pyrimidine units,[14] 2Md also shows strong absorption peaks at 496 nm and 618 nm even in the dilute solution of 10^{-6} mol/L (Figure 2c), suggesting the ultrastrong TSC between intramolecular pyrimidine units. These absorption peaks gradually increased with the increased concentration of solutions. We then studied their single-photon photoluminescence (PL) properties. Similar to many reported CLgens, these three CLgens are weakly emissive in the dilute solutions due to intramolecular molecular motions upon photoexcitation.[15] Nevertheless, long-wavelength emissions at 473 nm of 2Btz, 555 nm of 2Bxz, and 662 nm of 2Md could be detected in dilute solutions, respectively, indicating the appearance of CL caused by the intramolecular TSC (Figure S7). These emission peaks are excitation-dependent and become more dominant with the increased concentrations. In the crystalline state, 2Btz and 2Bxz show green and yellow CL with long-wavelength emission peaks at 476 nm and 560 nm and absolute quantum yields (QY) of 11% and 29%, respectively (Figure 2a and b). Unexpectedly, oily 2Md exhibits NIR emission at 688 nm with a QY of 19%, which is a new record of small-molecule CLgens (Figure 2c). It is noteworthy that their emission peaks are excitation-independent, suggesting the stabilization of TSC-based emission species in the solid and oily states (Figures S8 and S9). The decay curves of emission intensity within the nanosecond range support the fluorescent nature of their CL (Figure S10).

The long-wavelength emission and high QY compared to their isolated heteroatomic units indicate that *n*-electron-involved TSC endow these CLgens with a more substantial spatial conjugation effect for electron delocalization compared to pure π-electron CLgens. This excellent property encourages the investigation of their two-photon excited luminescence, which is traditionally observed in well-conjugated compounds. Surprisingly, all these CLgens display TPCL under NIR-II laser excitation with a broad two-photon excitation window of 900–1100 nm (Figure 2d–f). The emission peak of TPCL is almost the same as the steady-state CL at 525 nm of 2Btz, 566 nm of 2Bxz, and 668 nm of 2Md, respectively, proving the same processes from the excited state to the ground state under the one-photon and two-photon excitation.[16] To our knowledge, it is the first example of CLgens showing nonlinear optical properties and two-photon excited luminescence.

To further illustrate their photophysical properties, electronic structures and transitions were calculated based on the hole-electron analysis (Figure 3a). It is obvious that electrons are delocalized between two isolated heteroatomic units (pink arrow), suggesting the formation of typical intramolecular TSC.[7a] Besides, the lone-pair electrons from N atoms of 2Md directly overlap together, which should be responsible for its NIR CL and high QY. This result also supports the idea that introducing *n* electrons is an effective approach to enhancing TSC. The oscillator strength (*f*) and electric transition dipole moment (μ_{ge}) of each CLgens were further calculated in the aggregate model (Figure 3b), which are essential parameters for luminogens with two-photon luminescence. In particular, 2Bxz displays the largest value of *f* (0.5316) and μ_{ge} (5.745 Debye) due to its symmetric conformation and electron distribution in the excited state (Figure S11), indicating that it is a good candidate for TPCL materials.[17]

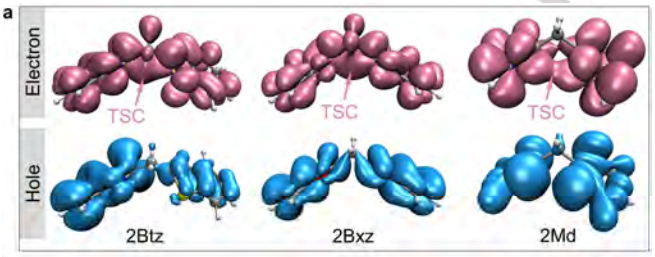

b

CLgen	λ_{ab} (nm)	λ_{TPCL} (nm)	QY (%)	*f*	μ_{ge} (Debye)
2Btz (solid)	295/401	525	11	0.0513	1.890
2Bxz (solid)	278/380	566	29	0.5316	5.745
2Md (oily)	284/496/618	688	19	0.0027	0.470

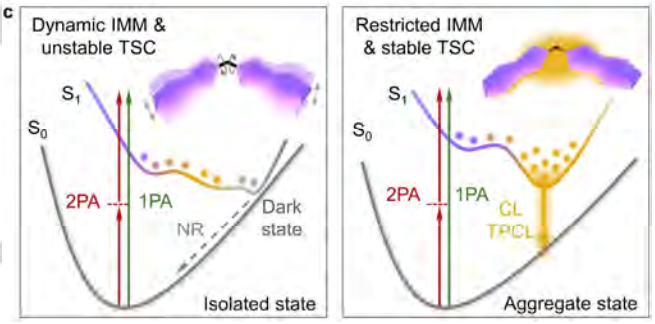

Figure 3. (a) Hole-electron analysis of 2Btz, 2Bxz, and 2Md in the aggregate state. (b) Summary of photophysical parameters of these three CLgens, including absorption (λ_{ab}) and TPCL (λ_{TPCL}) wavelength, absolute quantum yield (QY), and calculated oscillator strength (*f*) and electric transition dipole moment (μ_{ge}). (c) Schematic diagram of potential energy surfaces of CLgens in the isolated and aggregate states. 1PA = single-photon absorption, 2PA = two-photon absorption, NR = nonradiative decay.

Apart from intramolecular TSC, intermolecular interactions in the aggregate state also play an important role in promoting CL and TPCL properties of these CLgens. With the help of molecular dynamics calculation, the aggregate-state models of these three CLgens were obtained and compared with the single-molecule state (Figure S12). Reorganization energy (λ_{re}) was also calculated to indicate the geometry change between the optimized ground and excited state. As expected, intramolecular motion (IMM) of 2Btz and 2Bxz is violent, as evidenced by their large λ_{re} of 18929 cm^{-1} and 10422 cm^{-1}, respectively (Figures S13 and S14). In comparison, the λ_{re} value of 2Md (8497 cm^{-1}) is smaller, which is consistent with its strongest TSC and CL reaching the NIR region (Figure S15). After aggregation, the reduced λ_{re} value and proportion of dihedral-angle change to total

10.1002/anie.202413751

λ_{re} indicate that IMM is restricted due to multiple intermolecular interactions. In addition, multiple intermolecular interactions between heteroatoms (e.g., S···S, S···N of 2Btz, and N···O of 2Bxz) with shorter distances than intramolecular interactions are observed based on the single-crystal structures and Hirshfeld-surface analysis of 2Btz and 2Bxz (Figures S16-S19), proving their crucial role in the forming of intermolecular TSC and restricted IMM in the aggregate state.[18] Unfortunately, due to the oily state of 2Md, its crystal structure can not be obtained. Accordingly, Figure 3c illustrates the photophysical behaviors of these CLgens in isolated and aggregate states. In the isolated state, CLgens could form TSC after photoexcitation. However, dynamic IMM usually destroys TSC and leads to a dark state via nonradiative decay. In contrast, IMM is restricted in the aggregate state due to the confined environment and multiple intermolecular interactions, stabilizing formed TSC and promoting efficient CL under both one-photon and two-photon excitation.

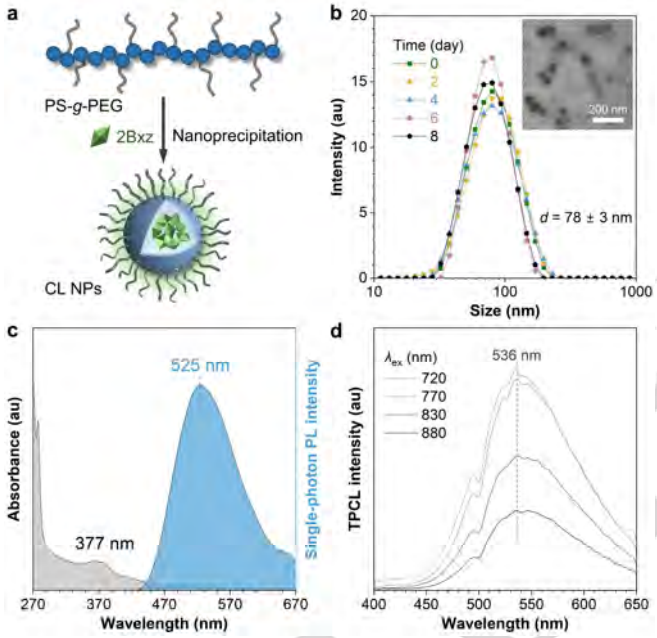

Figure 4. (a) Preparation of nanoparticles based on CLgens (CL NPs) using 2Bxz and PS-*g*-PEG. (b) Hydrodynamic size distributions of CL NPs solution stored at 4 °C for 8 days. Inset: TEM image of CL NPs. (c) Normalized UV-Vis absorption and single-photon PL spectra of CL NPs in solution. Excitation wavelength: 370 nm. (d) TPCL spectra of CL NPs solution under different excitation wavelengths.

Compared to largely conjugated luminogens, CLgens with simple and isolated units endow them with high biocompatibility and biodegradability, promoting them as a new type of bioprobes. Although 2Md shows the longest emission wavelength of TPCL, its fabricated nanoparticles exhibit low-quality bioimaging due to the oily state of 2Md and the poor stability of nanoparticles in the physiological environments (Figures S20 and S21), requiring further optimization. Nevertheless, with the highest QY, largest μ_{ge}, and excellent TPCL property, 2Bxz was also a good candidate and was selected as an example to investigate this potential biological application. Nanoparticles based on CLgens (CL NPs) of hydrophobic 2Bxz were fabricated via the nanoprecipitation method with poly(ethylene glycol) grafted polystyrene (PS-*g*-PEG) (Figure 4a). The size distribution and stability of the fabricated CL NPs were verified by the dynamic light scattering technique, which shows a consistent diameter of 78 nm for more than 1 week (Figure 4b). The transmission electron microscopy (TEM) image also proves their homogeneous spherical morphology. The photophysical properties of the fabricated CL NPs are similar to those of 2Bxz in the aggregate state, with the TSC-based absorption peak at 377 nm and PL emission at 525 nm, respectively (Figures 4c and S22). The TPCL emission also peaks at 536 nm with a two-photon excitation window of 720–880 nm within the NIR region, which is relatively blueshifted compared to the crystalline sample, probably due to irregular aggregates formed in nanoparticles (Figure 4d).

Encouraged by the excellent performance of the fabricated CL NPs, further investigation was carried out for *in vivo* angiography using BALB/c mice. The CL NPs in deionized water were injected into the tail vein and allowed to circulate within blood vessels. Under two-photon excitation of 830 nm, accompanied by the blue fluorescence of the second-harmonic generation (SHG) signal (within 415–485 nm) from surrounding collagen fibers, the blood vessels of the mouse ear show a bright green CL signal, which does not show an obvious change after several minutes (Figure 5a). The superior imaging quality can resolve the small blood vessel with a diameter of 18 μm, suggesting its high resolution. Besides, a 3D reconstruction imaging of blood vessels in the mouse ear was also performed *in vivo* by scanning the tissue of 37 μm depth to obtain a better spatial resolution and multi-dimensional information (Figure 5b).

Finally, the biocompatibility and biosafety of CL NPs were verified, which is another important parameter for CLgens as a new type of bioprobes. The weights of mice bodies and major organs (heart, lung, liver, kidney, and spleen) treated with CL NPs or phosphate-buffered saline (PBS) show no significant difference (Figure 5c-d). Besides, the histological study based on hematoxylin and eosin (H&E) staining displays that no obvious toxicity, such as neutrophil aggregation, tissue oedema, or microstructural damage, occurs in these major organs after treatment with CL NPs for 7 days, indicating excellent biocompatibility of the fabricated CL NPs (Figure 5e). To our knowledge, it is the first time that the CLgens were used for bioimaging *in vivo* with biocompatibility verification, which suggests that CLgens hold great promise as a new generation of bioprobes for biological applications.

In conclusion, three diarylmethane-based CLgens were designed and constructed by integrating heteroatomic rings. The *n*-electron-involved TSC endows them with long-wavelength CL (up to 688 nm) and high efficiency (up to 29%). Interestingly, TPCL was observed in CLgens without largely conjugated structures, which breaks the traditional cognition of two-photon fluorescent materials. Besides, these CLgens were successfully utilized for two-photon imaging of blood vessels *in vivo*, showing high resolution and good biocompatibility. This work highlights the essential role of TSC in promoting the nonlinear optical property of TPCL in CLgens and may open up new opportunities for developing the next-generation bioprobes.

10.1002/anie.202413751

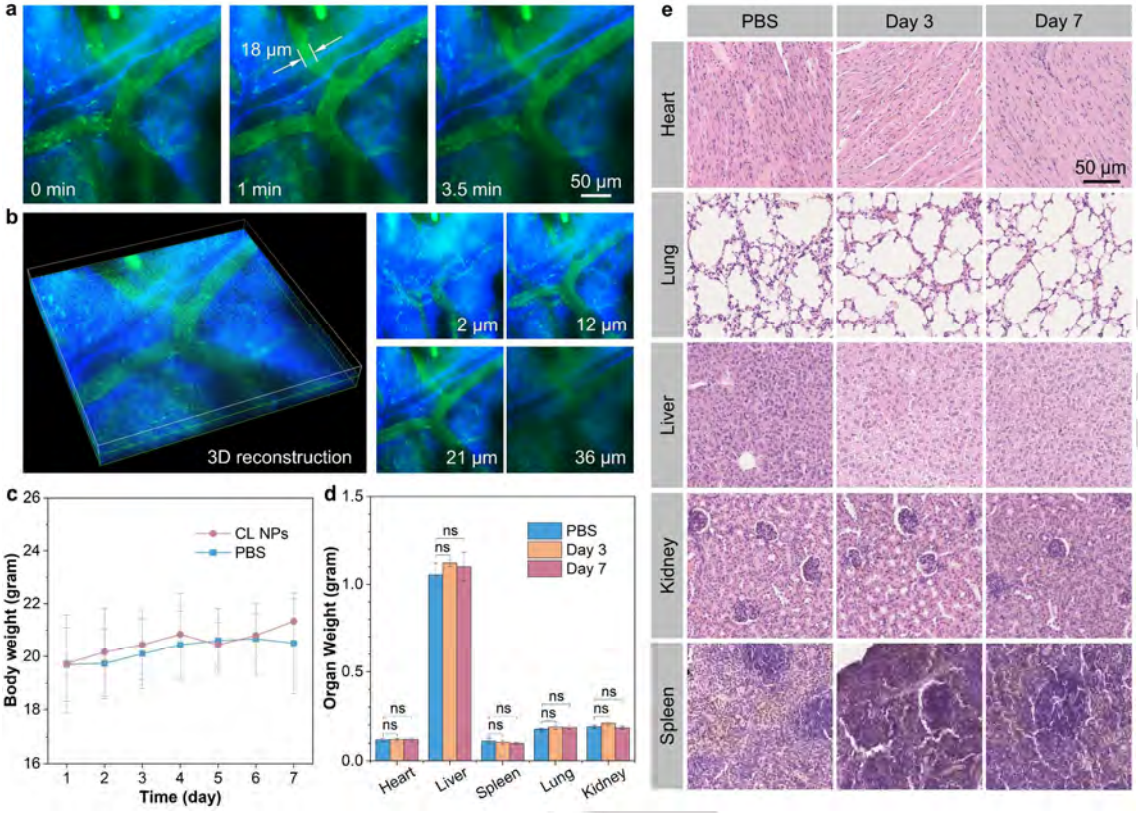

Figure 5. (a) Real-time imaging of mouse ear blood vessels under the two-photon microscope with the excitation wavelength of 830 nm after intravenous injection of CL NPs. Collection wavelength: 415–485 nm for the SHG signal of collagen fibers and 506–593 nm for the TPCL signal of CL NPs. (b) 3D reconstruction of mouse ear blood vessels. (c) The body weight in PBS (n = 3) and CL NPs groups collected at 24-hour intervals for 7 consecutive days. Data represent means ± standard deviation, n = 3. (d) The organ weights in three groups (PBS, Day 3, and Day 7). The statistical significance was calculated using the Student's T-test. ns = non-significant. (e) H&E staining of heart, lung, liver, kidney, and spleen. Mice were injected with CL NPs (1 mg/mL, 100 μL) via the tail vein, while the control group received an equal volume of PBS.

Acknowledgements

This work was supported by the National Natural Science Foundation of China Grant (22205197), the Fundamental Research Funds for the Central Universities (2024BSSXM04), the Research Grants Council of Hong Kong (16307020, C6014-20W and 16305320), the Innovation and Technology Commission (ITC-CNERC14SC01), and the Science and Technology Development Fund of Macau SAR (0049/2023/ITP2, 0003/2023/RIC and 0013/2023/RIC). J. Zhang acknowledges the support from the Marie Skłodowska-Curie Actions grant under the program of Horizon Europe (101105790). The authors thank the Animal Research Core in Faculty of Health Sciences, University of Macau.

Keywords: clusteroluminescence • through-space conjugation • nonlinear photophysics • two-photon fluorescence • bioimaging

[1] a) C. J. Weijer, *Science* **2003**, *300*, 96-100; b) P. van Roessel, A. H. Brand, *Nat. Cell Biol.* **2002**, *4*, E15-E20; c) D. W. Domaille, E. L. Que, C. J. Chang, *Nat. Chem. Biol.* **2008**, *4*, 168-175; d) Z. Chai, Q. Wu, K. Cheng, X. Liu, Z. Zhang, L. Jiang, X. Zhou, M. Liu, C. Li, *Angew. Chem. Int. Ed.* **2023**, *62*, e202300318; e) H. Fang, Y. Chen, Z. Jiang, W. He, Z. Guo, *Acc. Chem. Res.* **2023**, *56*, 258-269; f) R. Kubota, T. Hiroi, Y. Ikuta, Y. Liu, I. Hamachi, *J. Am. Chem. Soc.* **2023**, *145*, 18316-18328; g) X. Cui, Z. Zhang, Y. Yang, S. Li, C. Lee, *Exploration* **2022**, *2*, 20210264.

[2] a) S. Wang, W. X. Ren, J. Hou, M. Won, J. An, X. Chen, J. Shu, J. S. Kim, *Chem. Soc. Rev.* **2021**, *50*, 8887-8902; b) Z. Yang, A. Sharma, J. Qi, X. Peng, D. Y. Lee, R. Hu, D. Lin, J. Qu, J. S. Kim, *Chem. Soc. Rev.* **2016**, *45*, 4651-4667; c) Z. Li, P.-Z. Liang, T.-B. Ren, L. Yuan, X.-B. Zhang, *Angew. Chem. Int. Ed.* **2023**, *62*, e202305742; d) J. Zhang, J. Kan, Y. Sun, M. Won, J. H. Kim, W. Zhang, J. Zhou, Z. Qian, J. S. Kim, *ACS Appl. Bio Mater.* **2021**, *4*, 2080-2088; e) L. Wang, R. Chen, G. Han, X. Liu, T. Huang, J. Diao, Y. Sun, *Exploration* **2022**, *2*, 20210215.

[3] a) J. Nakai, M. Ohkura, K. Imoto, *Nat. Biotechnol.* **2001**, *19*, 137-141; b) A. Svendsen, H. V. Kiefer, H. B. Pedersen, A. V. Bochenkova, L. H. Andersen, *J. Am. Chem. Soc.* **2017**, *139*, 8766-8771; c) J. Kong, Y. Wang, W. Qi, M. Huang, R. Su, Z. He, *Adv. Colloid Interface Sci.* **2020**, *285*, 102286; d) A. Cao, Z. Ye, Z. Cai, E. Dong, X. Yang, G. Liu, X. Deng, Y. Wang, S. T. Yang, H. Wang, M. Wu, Y. Liu, *Angew. Chem. Int. Ed.* **2010**, *49*, 3022-3025.

[4] a) C. Coralli, M. Cemazar, C. Kanthou, G. M. Tozer, G. U. Dachs, *Cancer Res.* **2001**, *61*, 4784-4790; b) S. Cabantous, T. C. Terwilliger, G. S. Waldo, *Nat. Biotechnol.* **2005**, *23*, 102-107.

[5] a) S. Tang, T. Yang, Z. Zhao, T. Zhu, Q. Zhang, W. Hou, W. Z. Yuan, *Chem. Soc. Rev.* **2021**, *50*, 12616-12655; b) Z. Zhang, Z. Xiong, B. Chu, Z. Zhang, Y. Xie, L. Wang, J. Z. Sun, H. Zhang, X. H. Zhang, B. Z. Tang, *Aggregate* **2022**, *3*, e278; c) Z. Zhang, J. Zhang, Z. Xiong, B. Chu, C. Zhang, J. Z. Sun, H. Zhang, X. H. Zhang, B. Z. Tang, *Angew. Chem. Int. Ed.* **2023**, *62*, e202306762; d) C. Y. Shi, D. D. He, B. S. Wang, Q. Zhang, H. Tian, D. H. Qu, *Angew. Chem. Int. Ed.* **2023**, *62*, e202214422.

[6] a) Z. Zhang, L. Zhu, J. Feng, H. Zhang, X. Zhang, J. Z. Sun, B. Z. Tang, *Mater. Chem. Front.* **2023**, *7*, 713-719; b) A. Uva, S. Michailovich, N. S. Y. Hsu, H. Tran, *J. Am. Chem. Soc.* **2024**, *146*, 12271-12287; c) A. A. Mathew, M. Balachandran, *J. Inorg. Organomet. Polym. Mater.* **2023**, *33*, 3340-3354. d) Y. Zhang, J. Yuan, J. Hu, Z. Tian, W. Feng, H. Yan, *Aggregate* **2024**, *5*, e404.

10.1002/anie.202413751

[7] a) J. Zhang, L. Hu, K. Zhang, J. Liu, X. Li, H. Wang, Z. Wang, H. H. Y. Sung, I. D. Williams, Z. Zeng, J. W. Y. Lam, H. Zhang, B. Z. Tang, *J. Am. Chem. Soc.* **2021**, *143*, 9565-9574; b) H. Zhang, B. Z. Tang, *JACS Au* **2021**, *1*, 1805-1814; c) R. Hoffmann, *Acc. Chem. Res.* **1971**, *4*, 1-9; d) J. Sturala, M. K. Etherington, A. N. Bismillah, H. F. Higginbotham, W. Trewby, J. A. Aguilar, E. H. C. Bromley, A. J. Avestro, A. P. Monkman, P. R. McGonigal, *J. Am. Chem. Soc.* **2017**, *139*, 17882-17889; e) A. N. Sussardi, G. F. Turner, J. G. Richardson, M. A. Spackman, A. T. Turley, P. R. McGonigal, A. C. Jones, S. A. Moggach, *J. Am. Chem. Soc.* **2023**, *145*, 19780-19789; f) M. Lian, Y. Mu, Z. Ye, Z. Lu, J. Xiao, J. Zhang, S. Ji, H. Zhang, Y. Huo, B. Z. Tang, *Aggregate*, **2024**, *5*, e560; g) Y. Wang, J. Zhang, Q. Xu, W. Tu, L. Wang, Y. Xie, J. Z. Sun, F. Huang, H. Zhang, B. Z. Tang, *Nat. Commun.* **2024**, *15*, 6426.

[8] a) L. Wang, Z. Xiong, J. Zhi Sun, F. Huang, H. Zhang, B. Z. Tang, *Angew. Chem. Int. Ed.* **2024**, *63*, e202318245; b) R. Wang, W. Yuan, X. Zhu, *Chin. J. Polym. Sci.* **2015**, *33*, 680-687; c) A. Braendle, A. Perevedentsev, N. J. Cheetham, P. N. Stavrinou, J. A. Schachner, N. C. Mösch-Zanetti, M. Niederberger, W. R. Caseri, *J. Polym. Sci., Part B: Polym. Phys.* **2017**, *55*, 707-720.

[9] a) X. Liu, B. Chu, Z. Xiong, B. Liu, W. Tu, Z. Zhang, H. Zhang, J. Z. Sun, X. Zhang, B. Z. Tang, *Mater. Horiz.* **2024**, *11*, 1579-1587; b) Z. Zhang, H. Zhang, M. Kang, N. Li, D. Wang, B. Z. Tang, *Sci. China Chem.* **2021** 64, 1990-1998; c) H. Li, Y. Chen, H. Wang, H. Wang, Q. Liao, S. Han, Y. Li, D. Wang, G. Li, Y. Deng, *Adv. Funct. Mater.* **2023**, *33*, 2302862.

[10] a) J. Shin, P. Verwilst, H. Choi, S. Kang, J. Han, N. H. Kim, J. G. Choi, M. S. Oh, J. S. Hwang, D. Kim, I. Mook-Jung, J. S. Kim, *Angew. Chem. Int. Ed.* **2019**, *58*, 5648-5652; b) A. Podder, M. Won, S. Kim, P. Verwilst, M. Maiti, Z. Yang, J. Qu, S. Bhuniya, J. S. Kim, *Sens. Actuators B Chem.* **2018**, *268*, 195-204; c) Y. X. Wu, D. Zhang, X. Hu, R. Peng, J. Li, X. Zhang, W. Tan, *Angew. Chem. Int. Ed.* **2021**, *60*, 12569-12576; d) H. Shen, L. Du, C. Xu, B. Wang, Q. Zhou, R. Ye, R. T. K. Kwok, J. W. Y. Lam, G. Xing, J. Sun, T.-M. Liu, B. Z. Tang, *ACS Nano* **2024**, *18*, 20268-20282.

[11] a) S. R. Marder, *MRS Bulletin* **2016**, *41*, 53-62; b) M. Pawlicki, H. A. Collins, R. G. Denning, H. L. Anderson, *Angew. Chem. Int. Ed.* **2009**, *48*, 3244-3266; c) L. Xu, W. Lin, B. Huang, J. Zhang, X. Long, W. Zhang, Q. Zhang, *J. Mater. Chem. C* **2021**, *9*, 1520-1536; d) L. Wu, J. Liu, P. Li, B. Tang, T. D. James, *Chem. Soc. Rev.* **2021**, *50*, 702-734; e) T. B. Ren, W. Xu, Q. L. Zhang, X. X. Zhang, S. Y. Wen, H. B. Yi, L. Yuan, X. B. Zhang, *Angew. Chem. Int. Ed.* **2018**, *57*, 7473-7477; f) L. Zhang, Y. Zhou, M. Jia, Y. He, W. Hu, Q. Liu, J. Li, X. Xu, C. Wang, A. Carlsson, S. Lazar, A. Meingast, Y. Ma, J. Xu, W. Wen, Z. Liu, J. Cheng, H. Deng, *Matter* **2020**, *2*, 1049-1063.

[12] R. Passerini, *J. Chem. Soc.* **1954**, 2256-2261.

[13] a) B. He, J. Zhang, J. Zhang, H. Zhang, X. Wu, X. Chen, K. H. S. Kei, A. Qin, H. H. Y. Sung, J. W. Y. Lam, B. Z. Tang, *Adv. Sci.* **2021**, 2004299; b) Y. Morisaki, S. Ueno, A. Saeki, A. Asano, S. Seki, Y. Chujo, *Chem. Eur. J.* **2012**, *18*, 4216-4224.

[14] B. Samir, C. Kalalian, E. Roth, R. Salghi, A. Chakir, *Chem. Phys. Lett.* **2020**, *751*, 137469.

[15] a) H. Zhang, X. Zheng, N. Xie, Z. He, J. Liu, N. L. C. Leung, Y. Niu, X. Huang, K. S. Wong, R. T. K. Kwok, H. H. Y. Sung, I. D. Williams, A. Qin, J. W. Y. Lam, B. Z. Tang, *J. Am. Chem. Soc.* **2017**, *139*, 16264-16272; b) J. Zhang, P. Alam, S. Zhang, H. Shen, L. Hu, H. H. Y. Sung, I. D. Williams, J. Sun, J. W. Y. Lam, H. Zhang, B. Z. Tang, *Nat. Commun.* **2022**, *13*, 3492; c) Z. Xiong, J. Zhang, J. Z. Sun, H. Zhang, B. Z. Tang, *J. Am. Chem. Soc.* **2023**, 145, 21104–21113.

[16] H. Jin, M. Yang, Z. Sun, R. Gui, *Coord. Chem. Rev.* **2021**, *446*, 214114; b) A. Diaspro, G. Chirico, M. Collini, *Q. Rev. Biophys.* **2005**, *38*, 97-166.

[17] a) E. F. Petrusevich, M. Głodek, M. A. Antoniak, T. Muzioł, D. Plażuk, A. Siomra, M. Nyk, B. Ośmiałowski, R. Zaleśny, *Spectrochim. Acta A Mol. Biomol. Spectrosc.* **2023**, *295*, 122600; b) C. L. Sun, J. Li, X. Z. Wang, R. Shen, S. Liu, J. Q. Jiang, T. Li, Q. W. Song, Q. Liao, H. B. Fu, J. N. Yao, H. L. Zhang, *Chem* **2019**, *5*, 600-616.

[18] a) D.-R. Dauer, D. Stalke, *Dalton Trans.* **2014**, *43*, 14432-14439; b) Z. Xiong, J. Zhang, Z. Zhang, L. Wang, S. Wei, X. Liu, J. Z. Sun, H. Zhang, B. Z. Tang, *ACS Materials Lett.* **2024**, *6*, 3941-3950. c) Y. Tu, Z. Zhao, J. W. Y. Lam, B. Z. Tang, *Natl. Sci. Rev.* **2020**, *8*, nwaa260; d) J. Zhang, H. Zhang, J. W. Y. Lam, B. Z. Tang, *Chem. Res. Chin. Univ.* **2021**, *37*, 1-15; e) H. Shen, H. Wang, J. Mo, J. Zhang, C. Xu, F. Sun, X. Ou, X. Zhu, L. Du, H. Ju, R. Ye, G. Shi, R. T. K. Kwok, J. W. Y. Lam, J. Sun, T. Zhang, S. Ning, B. Z. Tang, *Bioactive Materials* **2024**, *37*, 299-312.

10.1002/anie.202413751

WILEY-VCH

COMMUNICATION

Entry for the Table of Contents

Two-photon clusteroluminescence (with emission wavelength up to 688 nm) was achieved in small clusteroluminogens (CLgens) with only two isolated heteroatomic units through the efficient and *n*-electron-involved through-space conjugation, which promotes the *in vivo* bioimaging of CLgens with excellent biocompatibility.

Institute and/or researcher Twitter usernames: @BenZhongTANG1, @HaokeZhang, @Jianyu_Zhang95, @ZJU_China, @HkustSc, @cuhksz